

Interannual variability in the CO₂ balance of a boreal patterned fen, James Bay, Canada

Noémie Cliche Trudeau · Michelle Garneau ·
Luc Pelletier

Received: 9 November 2012 / Accepted: 8 December 2013 / Published online: 14 January 2014
© Springer Science+Business Media Dordrecht 2014

Abstract During 2 years (2009, 2010), CO₂ fluxes were measured in an oligotrophic fen located at the ecotonal limit of forest tundra and lichen woodland, in northeastern Canada. Peatlands in this region have registered a rise in surface moisture since Little Ice Age, allowing an increase in their pool size and density. In the studied peatland, 83 % of the surface is covered either with pools (42 %), hollows (28 %) and lawns (13 %) all of which present a mean water table higher than 7 cm. We evaluated how these conditions might influence the CO₂ balance in these poor fens located in the northeastern section of the La Grande river watershed. During the two years measurements, results indicate a net CO₂ source with 404 (±287) and 272 (±250) g CO₂ m⁻² year⁻¹ emitted to the atmosphere throughout the growing seasons and winters. Modeled wintertime net ecosystem exchange resulted in a net loss of 150 (±36) and 150 (±37) g CO₂ m⁻² year⁻¹ in 2009 and 2010 respectively, while

248 (±248) and 124 (±195) g CO₂ m⁻² was emitted during 2009 and 2010 growing seasons. This high CO₂ source can be attributed to three factors: (1) the length of the cold season which represented 210–214 days of net CO₂ loss (2) a high pool/vegetated surface ratio since pools are a net source of CO₂ and presented 38–40 % of the annual spatially weighted CO₂ budget and (3) hydroclimatic conditions during the growing season as dryer and warmer conditions in 2009 reduced photosynthesis and increased respiration rates.

Keywords Aqualysis · Carbon dioxide · Fen · Pools · Methane · Annual balance

Introduction

In peatlands, carbon dioxide (CO₂) is absorbed by vegetation via photosynthesis and released through both autotrophic and heterotrophic respiration. Net ecosystem exchange (NEE) represents the difference between gross primary productivity (GPP) and ecosystem respiration (R). As net primary production generally exceeds decomposition in peatlands, these ecosystems are considered as carbon sinks. In a recent paper, Yu et al. (2010) estimated that northern peatlands stock represents 473–621 Gt C while MacDonald et al. (2006) showed that peat initiation and development contributed to reduce atmospheric CO₂ by 7 ppmv between 11 and 8 ka which

Responsible Editor: James Sickman

N. Cliche Trudeau (✉) · M. Garneau · L. Pelletier
GEOTOP-Geochemistry and Geodynamics Research
Center and Department of Geography, Université du
Québec à Montréal, Montreal, QC, Canada
e-mail: noemie14@hotmail.com

L. Pelletier
Department of Natural Resource Sciences, McGill
University, Sainte-Anne-de-Bellevue, Montreal, QC,
Canada

corresponded to a net cooling of -0.2 to 0.5 W m^{-2} (Frolking and Roulet 2007).

However, peatlands can also behave as a source of carbon. Silvola et al. (1996) have assessed that 90 % of the absorbed carbon in peatlands is released to the atmosphere over a year period. The small difference between absorbed and released CO_2 combined with peatlands sensitivity to hydro-climatic changes can lead to switch the peatlands' CO_2 budget from sink to source (Joiner et al. 1999; Cox et al. 2000; Griffis et al. 2000; Roulet et al. 2007). Moreover, the surface microtopography (hummock, lawn, hollow and pool) can influence the CO_2 balance of a peatland. Pelletier et al. (2011) showed NEE response to water table fluctuations where higher water table led to increased NEE in hummocks but reduced NEE in hollows. Open water bodies also contribute to the CO_2 budget (Waddington and Roulet 1996). In pools, Respiration in pools is mostly the result of organic matter decomposition (Kling et al. 1991; Hamilton et al. 1994; McEnroe et al. 2009). Moreover, CO_2 uptake by photosynthesis is limited and generally offset by CO_2 release to the atmosphere (Hamilton et al. 1994; Waddington and Roulet 1996; Macrae et al. 2004).

While several studies have demonstrated the response of peatlands to warmer and dryer conditions (Bubier et al. 2003a; Strack et al. 2006), the present research focuses in a peatland of northeastern Canada, where an overall rise of the regional water tables has been registered since the past 700 years (Arlen-Pouliot 2009; Van Bellen et al. 2013). This long-term disequilibrium of the hydrologic conditions generated gradual decomposition of strings and coalescence of pools. We refer to this phenomenon by the neologism 'aqualysis' (Dissanska et al. 2009; Proulx-McInnis et al. 2012; Trudeau et al. 2013). The main objective of this study was to evaluate the carbon balance of a peatland located at the ecotonal limit of the forest tundra and lichen woodland and to understand how a high general water table and pool coverage may play a role in this budget during two years. To understand the role of the hydrologic disequilibrium over carbon balance and as recent Canadian regional climate model (CRCM) outputs suggest future temperature and precipitation increase in this region of Canada (de Elia and Côté 2010), we analysed the influence of environmental variables such as water table on maximum rate of photosynthesis (PSN_{max}) and respiration (R) at microform scale and generated a two-year

overall carbon budget using measured and modelled CO_2 and CH_4 flux data.

Materials and methods

Study area and site

This study took place in the Northeastern region of the La Grande river watershed, James Bay, Québec (Fig. 1). Located at the ecotonal limit of forest tundra and lichen woodland, the region is sitting on Precambrian rocks, mostly granite and gneiss that were shaped by the last glaciation. Post glacial deposits such as till, esker, drumlins and moraines can be observed throughout the area (Dyke and Prest 1987). Characterised by acidic and poor soils, dominant vegetation of the region is represented by black spruce (*Picea mariana* (Mill) BSP) and lichens of the genus *Cladina* and *Cladonia* typical of the bioclimatic region of the lichen woodland (Payette et al. 2000). The area is under a subarctic climate with as mean annual temperature of $-4.28 \text{ }^\circ\text{C}$ and mean annual precipitation of 738 mm between 1971 and 2003 (Hutchinson et al. 2009) (Fig. 3). These characteristics lead to low evapotranspiration which favours high water table in the region and a high peatland cover (15 %), most of which are represented by oligotrophic patterned fen (Tarnocai et al. 2002).

The study site, chosen in 2008 on the basis of air and ground regional survey and landscape characterisation, is a 3.5 ha oligotrophic patterned fen. Abeille peatland ($54^\circ06.9'\text{N}$, $72^\circ30.1'\text{W}$) is formed by two distinct sections and one large pool downstream, close to the outlet (Fig. 2). It is characterised by elongated pools interspersed by strings perpendicular the general direction of the slope (Fig. 2). Pools cover 42 % of the total peatland area and their size vary between 4 and 99 m^2 while peat depth ranges between 10 and 300 cm with an average of 108 cm (Proulx-Mc Innis 2010). The vegetation of the peatland is largely dominated by sedges (*Carex exilis*, *C. Oligosperma* and *C. limosa*) but seven terrestrial microforms characterised by different water table depth, peat temperature and vegetation assemblage were identified along with two types of pools (Tables 1, 2, 3). Evidences of aqualysis were observed in the Abeille peatland under the form of eroded hummocks, of a diminution of the area covered by trees such as *Picea mariana* and *Larix*

Fig. 1 Study area and localisation of the peatland following Payette and Rochefort (2001) classification. The studied region (red circle) is located at the ecotonal limit between FO open boreal forest and TF forest tundra biomes

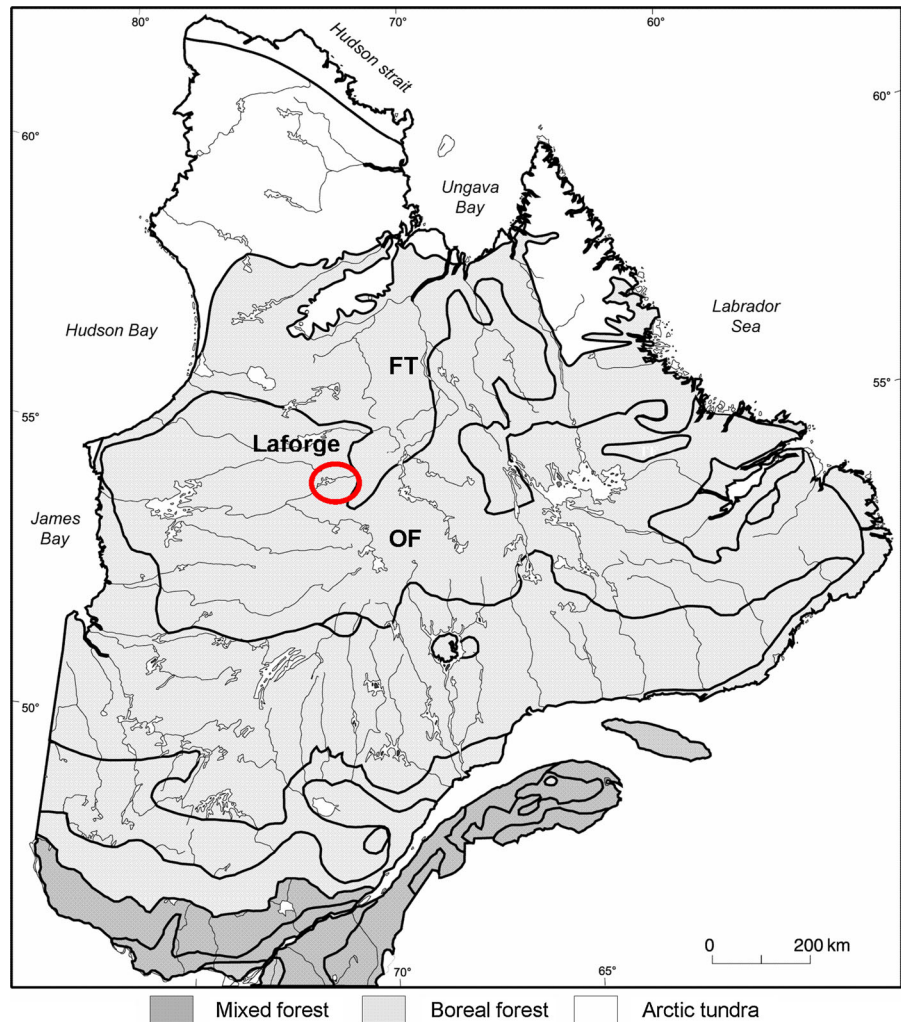


Fig. 2 Satellite image of Abeille peatland (May 18, 2010)

laricina and by a degradation of strings thus allowing pool fusion by coalescence. Traces of former strings were also observed in the center of some pools.

CO₂ flux measurements

CO₂ terrestrial fluxes measurements

In June 2009, seven representative terrestrial microforms were identified in the peatland (Tables 1, 2) and two collars (25 cm diameter) were installed in each one of them. As some of them showed similar characteristics (water table depth, peat temperature, vegetation assemblage), we combined microforms into three subgroups at time of analysis; lawns (six collars grouping *Cyperaceae* strings, *Cyperaceae*

Table 1 Microsites vegetation composition

Microsites	Vegetation
Hollows	
1	<i>Sphagnum cuspidatum</i> , <i>Gymnocolea inflata</i> , <i>Vaccinium oxycoccos</i> , <i>Menyanthes trifoliata</i> , <i>Carex limosa</i> , <i>Carex oligosperma</i>
2	<i>S. cuspidatum</i> , <i>G. inflata</i> , <i>V. oxycoccos</i> , <i>M.</i> <i>trifoliata</i> , <i>C. limosa</i> , <i>C. oligosperma</i> , <i>Cassandra calyculata</i>
Lawns	
3	<i>G. inflata</i> , <i>V. oxycoccos</i> , <i>Aster nemoralis</i> , <i>Kalmia</i> <i>polifolia</i> , <i>Andromeda glauca</i> , <i>C. calyculata</i>
4	<i>G. inflata</i> , <i>V. oxycoccos</i> , <i>Drosera rotundifolia</i> , <i>Coptis groenlandica</i> , <i>M. trifoliata</i> , <i>A.</i> <i>nemoralis</i> , <i>Carex exilis</i> , <i>Rhynchospora alba</i> , <i>Trichophorum cespitosum</i> , <i>K. polifolia</i> , <i>A.</i> <i>glauca</i> , <i>C. calyculata</i>
5	<i>S. cuspidatum</i> , <i>V. oxycoccos</i> , <i>D. rotundifolia</i> , <i>M.</i> <i>trifoliata</i> , <i>Smilacina trifolia</i> , <i>A. nemoralis</i> , <i>C.</i> <i>limosa</i> , <i>C. oligosperma</i> , <i>K. polifolia</i> , <i>A. glauca</i> , <i>C. calyculata</i> .
Hummocks	
6	<i>Sphagnum fuscum</i> , <i>V. oxycoccos</i> , <i>M. trifoliata</i> , <i>S.</i> <i>trifolia</i> , <i>C. oligosperma</i> , <i>K. polifolia</i> , <i>C.</i> <i>calyculata</i>
7	<i>S. fuscum</i> , <i>V. oxycoccos</i> , <i>Empetrum nigrum</i> , <i>Rubus chamaemorus</i> , <i>S. trifolia</i> , <i>C. limosa</i> , <i>C.</i> <i>oligosperma</i> , <i>K. polifolia</i> , <i>Ledum</i> <i>groenlandicum</i> , <i>C. calyculata</i> , <i>Picea mariana</i>

Table 2 Above ground biomass (end of 2010), water table depth (2009 and 2010) and peat temperature (2009 and 2010) for terrestrial microforms

Microsites	Above ground biomass (g/m ²)	Water table depth (cm)		Peat temperature (°C)	
		2009	2010	2009	2010
Hollows					
1	47.3	1.9	1.5	13.8	11.7
2	137.4	5.2	3.4	15.8	14.4
Lawns					
3	106.6	7.2	6.7	15.1	13.7
4	183.8	8.8	7.7	15.8	14.4
5	155.3	6.6	5.6	13.5	12.7
Hummocks					
6	682.9	24.7	24.9	14.9	13.1
7	793.2	20.4	17.8	10.4	10.0

lawns and *Sphagnum* lawns), hummocks (four collars grouping hummocks and the forest borders) and hollows (four collars grouping pool borders and

Table 3 Depth, dimension and vegetation composition of the pools

Pools	Depth	Dimensions (center)	Vegetation composition
Shallow pool	36–43 cm	5 × 13 m	<i>Sphagnum cuspidatum</i> , <i>Menyanthes trifoliata</i> , <i>Andromeda glauca</i> , <i>Kalmia polifolia</i>
Deep pool	75–95 cm	10 × 20 m	<i>Menyanthes trifoliata</i> , <i>Nuphar lutea</i> , <i>Andromeda glauca</i>

hollows). Two pools respectively shallow (39.7 cm) and deep (78.5 cm) were also chosen for sampling (Table 3). Spatial microform coverage obtained with Geo Eye imagery classification (Dribault et al. 2012) show that the peatland is mainly represented by pools (42 %) and terrestrial microforms with water table close to peat surface such as hollows and lawns (41 %) while hummocks represent only a minor proportion of the peatland (17 %). To reduce the impacts of sampling, boardwalks were installed between the sites. NEE was measured during 6 field campaigns spread over two growing seasons. In 2009, three field campaigns were carried out in July, August and October while in 2010 three field campaigns were carried out in June, July and August respectively. Each campaign included 10 days of daily measurements.

During each campaign, CO₂ fluxes were measured every day using a closed system composed of a climate-controlled static chamber connected to an infrared gas analyser (*PPsystems EGM-4*, Massachusetts, USA) placed on plastic collars. The 18L Plexiglas chamber transmitted about 92 % of the photosynthetically active radiation (PAR) and had a removable top in order to re-establish the ambient conditions between the measurements. It also had a climate-control system consisting in a fan and a pump immersed in cold water allowing water circulation in a radiator to maintain temperature inside the chamber close to ambient.

At the time of measurement, the chamber was placed on the collar with a water seal. We monitored the change in CO₂ concentration in the chamber over a 2.5-min period, recording one data every 10 s for the first minute and one data every 30 s for the last 1.5 min. The CO₂ flux was calculated from linear regression using the CO₂ concentration change during

the 2.5-min period. We also measured photosynthetically active radiation (*PAR-1 sensor, PP Systems*) during the fluxes sampling. Shrouds with different mesh size, partly blocking the incoming PAR, were used to create different light intensities. In each collar, 4 measurements were conducted, the first one at full light, then blocking 25 and 50 % of the light and using an opaque shroud to measure respiration.

CO₂ pool fluxes measurements

Open water pools were sampled for CO₂ and CH₄ concentrations every two days during the field campaigns following Hamilton et al. (1994). Water samples were taken in glass bottles (Wheaton 125 mL) sealed with a rubber septum. The bottles were previously prepared in laboratory by (1) adding 8.9 g of KCl in order to inhibit water biological activity, (2) removing the air contained in the bottle with a vacuum pump and (3) adding 10 mL of UHP N₂ to the bottle to create a headspace. In the field, as the air from the bottle was removed beforehand, samples were taken by submerging the bottle in water and by perforating the septum with a 18 gauge needle until filled. At sampling time, air and water temperature as well as wind speed were measured in order to be included in Eqs. 2 and 5.

At analysis time, bottles were shaken for 3 min to equilibrate water and N₂. Using a 12 gauge needle, the headspace was sampled and analysed with a gas chromatograph (*Shimadzu GC-14B*) to determine CO₂ partial pressure (Hamilton et al. 1994; Demarty et al. 2009). As a dissolved gas concentration in a solution is directly proportional to this gas partial pressure in the solution, Henry's law was used to calculate CO₂ concentration (Hamilton et al. 1994) using Eqs. 1 and 2:

$$\text{CO}_2\text{wc} = K_{\text{H}}(\text{CO}_2) * \text{CO}_2\text{wp} \quad (1)$$

$$K_{\text{H}}(\text{CO}_2) = -58,0931 + 90,5069(100/T_{\text{K}}) + 22,294 * \ln(T_{\text{K}}/100) \quad (2)$$

where CO₂wc is CO₂ concentration in the water; CO₂wp is CO₂ partial pressure; K_H(CO₂) is CO₂ solubility in water in mol L⁻¹ atm⁻¹; T_K is water temperature in Kelvin

CO₂ fluxes were calculated using the «thin boundary layer» as described by Demarty et al. (2009) (Eq. 3).

$$F = k(\Delta C) \quad (3)$$

where:

$$F = k(\text{CO}_2\text{wc} - \alpha\text{CO}_2\text{ac})$$

where F is the gas flux at water/air interface; αCO₂ac is the gas concentration in water exposed to the atmosphere calculated with Eq. 2 and global mean atmospheric partial pressure of 383 for carbon dioxide. k is the gas exchange coefficient.

To be applied to CO₂ and ambient conditions, we adjusted k values with temperature, viscosity and CO₂ diffusion coefficients with the Schmidt number (obtained by dividing water kinematic viscosity at temperature a' by gas diffusion coefficient at temperature a') following Cole and Caraco (1998) (Eq. 4):

$$K_{600} = 2.07 + 0.215U_{10}^{1.7} \quad (4)$$

where K₆₀₀ is the exchange coefficient measured with sulphur hexafluoride (SF₆), normalized to Schmidt number (Sc number) of 600, which is the Sc number for SF₆ at 20 °C (Crusius and Wanninkhof 2003) and U₁₀ represents wind speed at 10 m.

Finally, k was calculated with the following equations (Crusius and Wanninkhof 2003) (Eqs. 5 and 6): If wind speed <3 m/sec:

$$k_{\text{CO}_2}(\text{cm/h}) = k_{600} \left(600^{0.66} / \text{Sc}_{\text{CO}_2}^{0.66} \right) \quad (5)$$

If wind speed ≥3 m/sec

$$k_{\text{CO}_2}(\text{cm/h}) = k_{600} \left(600^{0.50} / \text{Sc}_{\text{CO}_2}^{0.50} \right) \quad (6)$$

where k_{CO₂} is the gas coefficient exchange for CO₂ and Sc_{CO₂} is Schmidt number for CO₂

This method allowed us to measure CO₂ fluxes from the pools to the atmosphere. Considering that there is low photosynthetic activity in the pools (Hamilton et al. 1994; Macrae et al. 2004), we did not measure CO₂ invasion so the CO₂ contribution may be overestimated.

CH₄ measurements

CH₄ fluxes were measured every two days over the same range of microforms than for CO₂ sampling during 2009 and 2010 growing season (Trudeau et al.

2013). A 18L foil covered static chambers placed over collars sealed with water was used (Crill et al. 1988). CH₄ samples (4) were taken every 6 min for a 24-min period. Air inside the chamber was mixed using a 60 mL syringe and a sample was taken and injected in a 10 mL pre-evacuated glass vial sealed with a rubber septum (butyl 20 mm septa, Supelco cie.) and a metal crimp (Ullah et al. 2009). Samples were kept at 4 °C until analysis with a gas chromatograph (*Shimadzu GC-14B*) equipped with a flame ionization detector for CH₄. Fluxes were determined from a linear regression between the 4 measured CH₄ concentrations during the 24-min sampling. CH₄ fluxes from the pools were measured using the method described in the previous section, K_H(CH₄) being determined using the following equation (Eq. 7):

$$K_H(\text{CH}_4) = -115,6477 + (155.5756/(T_K/100)) + 65.2553 * \ln(T_K/100) - 6,1698 * (T_K/100) \quad (7)$$

where CH₄wc is CH₄ concentration in the water; CH₄wp is CH₄ partial pressure; K_H(CH₄) is CH₄ solubility in water in mol L⁻¹ atm⁻¹; T_K is water temperature in Kelvin

Environmental variables

In each microform, water table depth and peat temperature were monitored continuously between June 13th 2009 and September 1st 2010. Water table depth was measured using a level logger (*Odyssey Capacitance Water Level Logger*) placed in PVC tube and inserted into peat or pool bottom. Peat and water temperatures were measured using HOBO probes (*TMC6-HD Air/Water/Soil Temp Sensor*) inserted at different depths (5–10–20–40 cm) on the terrestrial microforms. In the pools, water temperature was measured at the center and along the border both in surface and at the bottom. Aboveground biomass was measured by clipping vegetation inside collars at the end of 2010 growing season. Vascular plants stems and leaves were sorted and only capitula were kept for *Sphagnum* species. Vegetation was then dried in the oven at 80 °C and weighted to calculate biomass (Moore et al. 2002). Meteorological data were monitored from meteorological station located in a nearby peatland (<1 km) for 2009 and in Abeille peatland for 2010.

Data analysis

The relationship between NEE and PAR was described by a rectangular hyperbola using a curve-fitting technique (Eq. 8) (Fig. 8) that was computed with JMP-IN statistical software (*SAS institute* 2007).

$$NEE = (\alpha * PAR * GP_{max} / (\alpha * PAR + GP_{max})) + R \quad (8)$$

where: α is the initial slope of the rectangular hyperbola (apparent quantum yield)

PAR is photosynthetically active radiation

GP_{max} is the maximum gross photosynthesis in light saturation condition

R is the intercept of the curve or dark respiration value

CO₂ uptake by the ecosystem is represented by positive signs and CO₂ release to the atmosphere by negative values.

The length of the growing season was defined using peat temperature at 5 cm to determine date of spring thaw and autumn freeze. We assumed that there was no photosynthetic activity when peat was frozen. The 2009 growing season lasted from May 12th to October 9th (151 days) and April 28th to September 30th (155 days) in 2010.

Rectangular hyperbola curve (Eq. 8) was fitted in the data of each sampling site for every field campaign (July, August and October 2009; June, July and August 2010) and the parameters estimated were applied to an hourly model of NEE. Gaps were filled between field campaigns using a mobile mean to estimate the rectangular hyperbola parameters. Table 4 shows seasonal estimates of the rectangular hyperbola parameters for 2009 and 2010. As the rectangular hyperbola tend to underestimate respiration values, R was modeled separately using an exponential regression derived from relationship between daily dark respiration measurements for 2 years and peat temperature at 5 cm (Table 5, Fig. 6).

Peat temperature was modeled between January 1st 2009 and June 11th 2009 and between September 1st 2010 and December 31st 2010 using an exponential regression with air temperature. We did not model pool fluxes as no strong relationship between water temperature and CO₂ emissions was detected. Thus, only the growing season budget includes pool emissions for which pool seasonal average fluxes (shallow

Table 4 Rectangular hyperbola parameters (Standard error in parenthesis) for NEE-PAR curves at each field campaigns as calculated with JMPin for the different microforms in 2009 and 2010. α values are in $\text{g CO}_2 \text{ m}^{-2} \text{ d}^{-1} / \mu\text{mol m}^{-2} \text{ s}^{-1}$

Microforms	Month, year	GP _{max}	PSN _{max}	α	R	N	r ²
Hollows	July 2009	11.50 (0.68)	9.61 (0.38)	0.04 (0.007)	-3.41 (0.31)	155	0.79
	August 2009	5.26 (0.41)	5.75 (0.27)	0.05 (0.015)	-0.76 (0.23)	192	0.59
	October 2009	0.56 (0.6)	–	0.001 (0.001)	-0.07 (0.06)	48	0.17
	June 2010	4.95 (0.71)	3.42 (0.4)	0.008 (0.002)	-1.09 (0.21)	127	0.53
	July 2010	6.31 (0.33)	5.53 (0.5)	0.03 (0.006)	-1.56 (0.16)	190	0.77
	August 2010	4.29 (0.38)	3.3 (0.43)	0.01 (0.002)	-0.92 (0.13)	135	0.71
Lawns	July 2009	24.29 (1.1)	19.11 (0.48)	0.05 (0.006)	-8.42 (0.41)	235	0.83
	August 2009	21.47 (1.46)	18.64 (0.62)	0.04 (0.005)	-3.91 (0.43)	206	0.77
	October 2009	3.81 (0.53)	–	0.02 (0.004)	-0.84 (0.12)	135	0.62
	June 2010	12.73 (0.84)	10.87 (0.49)	0.02 (0.003)	-3.24 (0.28)	239	0.71
	July 2010	21.7 (1.13)	15.7 (0.68)	0.04 (0.004)	-5.64 (0.31)	264	0.82
	August 2010	11.57 (0.95)	9.56 (1.07)	0.03 (0.006)	-1.89 (0.39)	89	0.77
Hummocks	July 2009	40.86 (2.42)	27.79 (0.99)	0.06 (0.007)	-17.13 (0.79)	191	0.81
	August 2009	41.88 (2.2)	32.33 (1.2)	0.09 (0.01)	-12.72 (0.77)	208	0.82
	October 2009	13.82 (1.56)	–	0.04 (0.007)	-3.98 (0.31)	125	0.74
	June 2010	22.79 (1.43)	5.36 (0.92)	0.07 (0.01)	-7.94 (0.63)	159	0.76
	July 2010	39.05 (1.92)	9.07 (1.42)	0.14 (0.02)	-14.64 (0.83)	208	0.82
	August 2010	78 (8.49)	3.17 (1.42)	0.07 (0.007)	-6.6 (0.77)	61	0.94

PSN_{max}, GP_{max} and R values are in $\text{g CO}_2 \text{ m}^{-2} \text{ d}^{-1}$

Table 5 Exponential regression equation, coefficient of determination (r²) probability (p) and sample size (n) values for relationship between 2009 and 2010 respiration ($\text{g m}^{-2} \text{ d}^{-1}$) and peat temperature at 5 cm (T5, °C) for each microform

Microform	Equation	p	r ²	n
Hollows	$y = 0.1448e^{0.1568T5}$	$p < 0.001$	0.35	209
Lawns	$y = 0.5629e^{0.1483T5}$	$p < 0.001$	0.44	317
Hummocks	$y = 3.1185e^{0.0994T5}$	$p < 0.001$	0.42	242

and deep) were used. For the yearly model we assumed that the pools stopped emitting CO₂ when an ice cover formed on the surface. However, no data are associated with the release following the ice melt in spring and therefore the annual pool contribution may be underestimated.

In order to identify the controlling factors of NEE, simple regressions (significance level = 0.05) were used. As NEE represents the difference between gross primary productivity (GPP) and respiration (R), we analysed the relationship between GPP and R and the environmental variables (water table depth, peat and water temperature and biomass) separately. As GP_{max} suggests an infinite limit of PAR, we used photosynthesis

values under real light saturation condition (PAR > 1,000 $\mu\text{mol m}^{-2} \text{ s}^{-1}$) (PSN_{max}) (Bubier et al. 2003a) for a more realistic analysis of photosynthesis. NEE_{max}, which represents the difference between gross primary productivity and respiration under light saturation condition (PAR > 1,000 $\mu\text{mol m}^{-2} \text{ s}^{-1}$) was also used for analysis. One way ANOVA tests (significance level = 0.05) were conducted to compare means between 2009 and 2010. Shapiro–Wilk test was used to determine normality of the distributions (significance level = 0.05) and Cook's distance was used to identify outliers. A total of 3,011 terrestrial fluxes were measured from which 2,994 were kept with 1,587 in 2009 and 1,407 in 2010. In the aquatic sites, 89 fluxes were kept out of 98 measured with 42 in 2009 and 47 in 2010.

The uncertainties associated with the data presented in this manuscript take into account the error associated with the derived relationships between fluxes and environmental variables (PAR, water table depth, temperature, biomass). However, numbers of errors that are hardly quantifiable are associated with the methods. The largest sources of probable error would derive from the measurement techniques and materials, from the assessment of an annual budget using

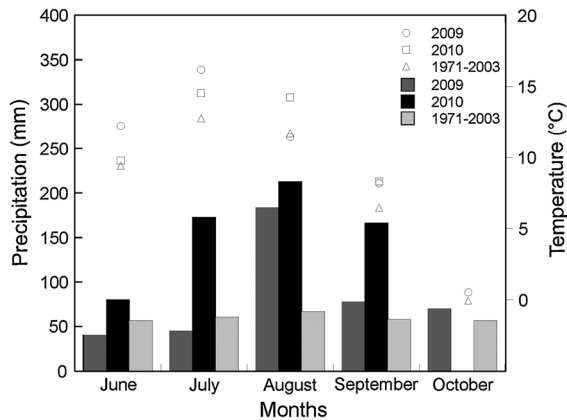


Fig. 3 Monthly average temperature (symbols, °C) and precipitation (bars, mm) in 2009, 2010 and 1971–2003 (Hutchinson et al. 2009)

non-continuous measurements (gap-filling) and from the scaling up of chamber measurements to the landscape level.

Results

Environmental conditions

Mean daily temperature between June 1st and September 1st was warmer than the 30 years average with 13.2 and 13 °C for 2009 and 2010 respectively (Fig. 3). For the same period, total precipitation was inferior to the 30 years mean (299 mm) in 2009 (269 mm) and exceeded the 30 years mean in 2010 (477 mm). In the hummocks, water table depth varied between -16.5 and -25.6 cm in the 2009 growing season and between -15.5 and -27.5 cm in 2010. In the lawns, water table depth ranged from -3.7 to -10.9 cm in 2009 and between -3.1 and -13.3 cm in 2010. In the hollows, water table depth varied between 0.2 and -6.2 cm in 2009 and between 0.9 and -9 cm in 2010. Lower precipitations during 2009 growing season did not lead to a large water table drawdown (Fig. 4) although the duration of the low precipitation period influenced *Sphagnum* surface desiccation on microforms with deeper water tables such as lawns and hummocks. This is consistent with Strack and Price (2009) observations which did not establish a constant direct correlation between water table depth and *Sphagnum* moisture content.

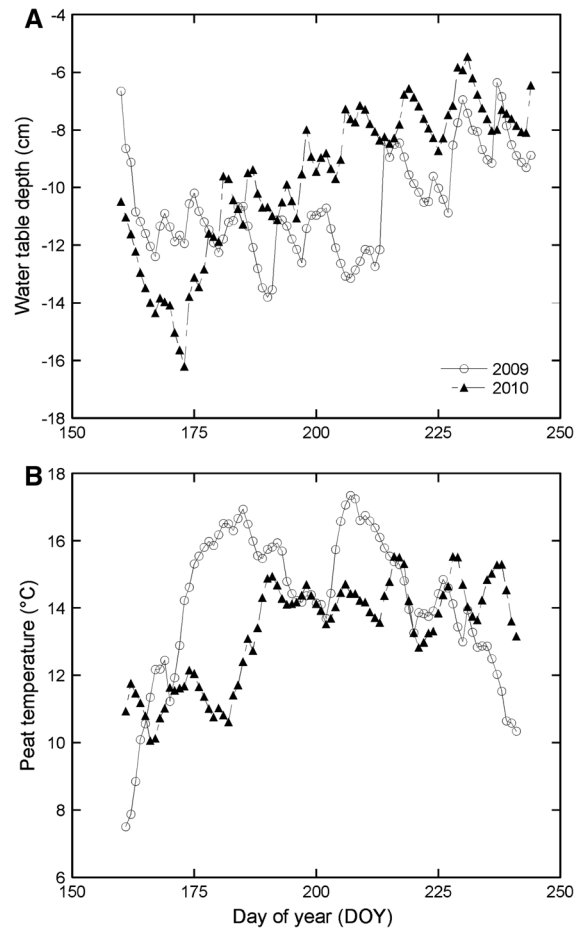


Fig. 4 2009 and 2010 seasonal pattern of mean peatland water table position (a) (0 = peat surface including moss cover) and peat temperature at 20 cm (b) from vegetated surface

Spatial variability

One-way ANOVA test performed on individual CO_2 fluxes measurements revealed that photosynthesis at $\text{PAR} > 1,000 \mu\text{mol m}^{-2} \text{s}^{-1}$ (PSN_{max}), net ecosystem exchange at $\text{PAR} > 1,000 \mu\text{mol m}^{-2} \text{s}^{-1}$ (NEE_{max}) and dark respiration (R) were significantly different between the microforms and during both years ($p > 0.001$).

The rectangular hyperbola curve parameters varied according to the microtopography sequence: hollow < lawn < hummock (Table 4). GP_{max} varied between 4.5 and $9.01 \text{ g CO}_2 \text{ m}^{-2} \text{ d}^{-1}$ in the hollows, between 15.75 and $18.75 \text{ g CO}_2 \text{ m}^{-2} \text{ d}^{-1}$ in the lawns and ranged from 31.98 to $32.2 \text{ g CO}_2 \text{ m}^{-2} \text{ d}^{-1}$ in the hummocks. Dark respiration varied from -1.29 to

$-1.6 \text{ g CO}_2 \text{ m}^{-2} \text{ d}^{-1}$ in the hollows, -4.33 and $-4.89 \text{ g CO}_2 \text{ m}^{-2} \text{ d}^{-1}$ in the lawns and -11.22 and -11.76 in the hummocks (Table 4). In the pools, CO_2 emissions ranged from -0.01 to $-10 \text{ g m}^{-2} \text{ d}^{-1}$ with a mean of $-2.3 (\pm 0.3)$. Shallow pool was a stronger emitter than deep pool with respective mean seasonal flux of -5.38 (0.6) and $-1.18 (\pm 0.2) \text{ g CO}_2 \text{ m}^{-2} \text{ d}^{-1}$ in 2009 and $-3.28 (\pm 0.6)$ and $0.78 (\pm 0.1) \text{ g CO}_2 \text{ m}^{-2} \text{ d}^{-1}$ in 2010.

Interannual variability

One-way ANOVA tests were performed to determine NEE_{max} , PSN_{max} and R statistical difference between 2009 and 2010 growing seasons in the terrestrial microforms (Fig. 5). For these tests, we used individual CO_2 measurements collected during July and August. In the hollows, NEE_{max} , PSN_{max} and R were significantly higher in 2009 than in 2010 ($p < 0.001$). In the lawns, NEE_{max} was statistically similar during 2009 and 2010 ($p = 0.101$) while PSN_{max} and R were significantly higher in 2009 ($p < 0.001$). In the hummock, NEE_{max} and PSN_{max} were significantly higher in 2010 ($p < 0.001$) but R was higher in 2009 ($p = 0.054$). Pool fluxes were significantly greater in 2009 in shallow pool ($p = 0.023$) but were similar in deep pool ($p = 0.089$) of both years.

Environmental controls

In order to identify the controls on NEE , relationship between CO_2 fluxes (PSN_{max} and R) and environmental variables (air temperature, peat temperature, water table depth and biomass) were established at seasonal and daily scale. Relationships were also determined at both ecosystem and microform scale (Table 6). R measurements were strongly correlated with water table depth, fluxes increasing with deeper water table. At the seasonal scale, water table depth explained 88 % ($p < 0.001$) of the respiration fluxes, a 25 cm decrease of the water table yielding fluxes about one order of magnitude higher. Fluctuations of the water table also showed a statistically significant relationship with respiration fluxes at the daily scale ($p < 0.001$; $r^2 = 0.55$). However, the strength of the relationship varied among microforms. Water table depth explained 30 % of R variation in hollows ($p < 0.001$) and 52 % in lawns ($p < 0.001$) while it correlated very weakly in hummocks ($r^2 = 0.06$;

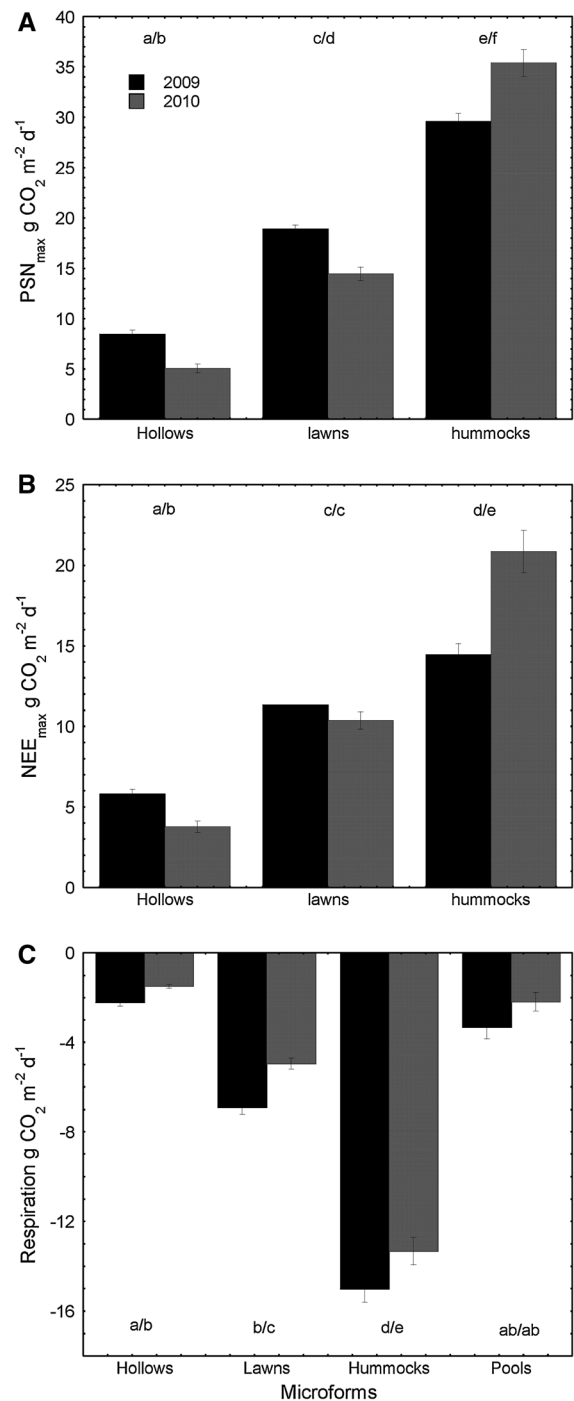


Fig. 5 Mean Respiration, PSN_{max} and NEE_{max} (\pm standard error) for June and July 2009 and 2010. Different letter indicates significant differences ($\alpha = 0.05$)

$p < 0.001$). Similar results for this relationship were obtained when 2009 and 2010 growing seasons were analysed separately. In pools, CO_2 fluxes were also

Table 6 Respiration and PSN_{max} regression parameters (r^2 , p value and sample size) for relationships with water table depth (WTD), air temperature (air temp.), peat temperature (peat temp) and biomass

Microform	Hummocks			Lawn			Hollow			Pool			Ecosystem		
	r^2	p	n	r^2	p	n	r^2	p	n	r^2	p	n	r^2	p	n
Daily R × WTD	0.06	0.001	242	0.52	0.001	317	0.30	0.001	209	0.39	0.001	77	0.55	0.001	768
Daily R × air temp	0.54	0.001	217	0.65	0.001	282	0.38	0.001	198	0.10	0.002	78	0.29	0.001	14
Daily PSN _{max} × WTD	0.02	0.4	192	0.18	0.001	211	0.34	0.001	117	-	-	-	0.58	0.001	520
Daily PSN _{max} × air temp	0.02	0.06	192	0.15	0.001	211	0.24	0.001	118	-	-	-	0.03	0.0002	521
Daily PSN _{max} × peat temp	0.03	0.013	192	0.17	0.001	211	0.47	0.001	118	-	-	-	0	0.291	521
Seasonal R × WTD	-	-	-	-	-	-	-	-	-	-	-	-	0.88	0.001	14
Seasonal R × air temp	-	-	-	-	-	-	-	-	-	-	-	-	0.29	0.001	14
Seasonal R × biomass	-	-	-	-	-	-	-	-	-	-	-	-	0.89	0.001	14
Seasonal PSN _{max} × WTD	-	-	-	-	-	-	-	-	-	-	-	-	0.83	0.001	14
Seasonal PSN _{max} × biomass	-	-	-	-	-	-	-	-	-	-	-	-	0.87	0.002	14

correlated with water levels ($r^2 = 0.39$; $p < 0.001$) with higher fluxes measured at lower water levels.

The relationship between PSN_{max} and water table depth was also analysed. At the ecosystem level, PSN_{max} was strongly correlated with water table depth at seasonal scale ($r^2 = 0.83$; $p < 0.001$) and also correlated at the daily scale ($r^2 = 0.58$; $p < 0.001$) with more CO₂ uptake with deeper water table. Similarly to respiration, a 25 cm decrease in the water table lead to fluxes about one order of magnitude higher. Daily measurements of CO₂ at the microform scale showed that water table explained 34 % of PSN_{max} variation in the hollows ($p < 0.001$), 18 % in lawns ($p < 0.001$) while the relationship was very weak in hummocks ($r^2 = 0.02$; $p = 0.042$).

A correlation between R fluxes and air temperature was observed at the daily scale for both years ($r^2 = 0.37$; $p < 0.001$ in 2009 and $r^2 = 0.19$; $p < 0.001$ in 2010), warmer temperature leading to higher fluxes. Within the microforms, the strongest relationship between individual R fluxes and air temperature was measured in lawns ($r^2 = 0.65$; $p < 0.001$), followed by hummocks ($r^2 = 0.54$; $p < 0.001$) and hollows ($r^2 = 0.38$; $p < 0.001$). A weak but significant relationship was also measured in pools ($r^2 = 0.10$; $p = 0.002$). R fluxes also varied according to peat temperature at 5 cm (closely correlated to air temperature) (Fig. 6). An exponential curve was fitted between R fluxes at the daily scale and peat temperature and explained 10 % of R variation within the ecosystem ($p < 0.001$). When considered at the microform scale, peat temperature explains 35 % of the variation of R fluxes in the hollows ($p < 0.001$), 44 % in the lawns ($p < 0.001$) and 42 % in the hummocks ($p < 0.001$) (Table 5). In pools (shallow and deep), water temperature at the border bottom explained 11 % of the variations ($p = 0.004$). The relationship was stronger in deep pool ($r^2 = 0.35$; $p = 0.004$) than in the shallow pool ($r^2 = 0.13$; $p = 0.014$). For each microform, the relationship between R fluxes and temperature (air and peat) was stronger during the dryer and warmer 2009 growing season.

PSN_{max} was also correlated to air temperature at the daily scale, warmer temperature leading to increasing uptake. However, the relationship is weaker than the one for R. Within the microforms, air temperature explained 24 % of PSN_{max} variation in the hollows ($p < 0.001$), 15 % in the lawns ($p < 0.001$) and the

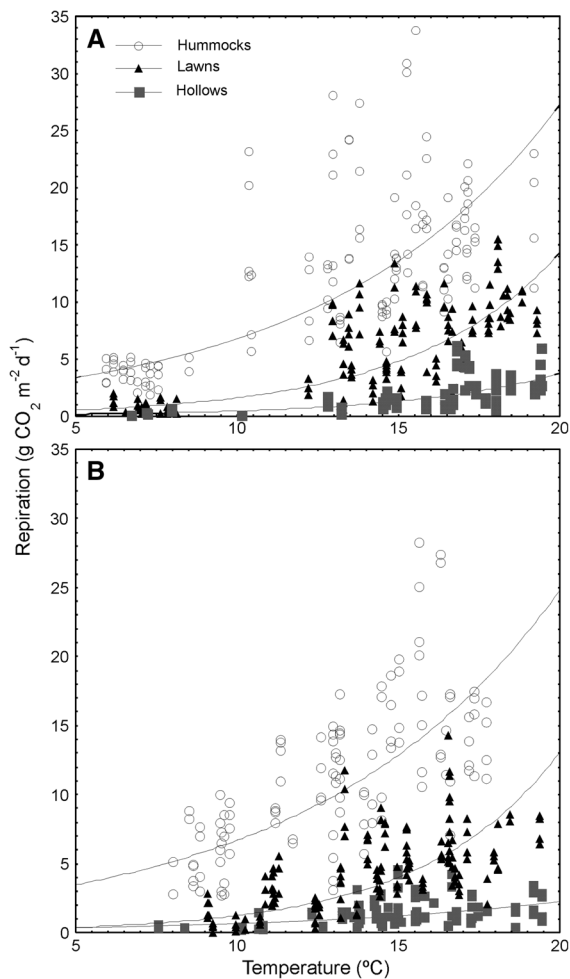


Fig. 6 Relationship between peat temperature at 5 cm and respiration in 2009 (a) and 2010 (b)

relationship was not significant in the hummocks ($p = 0.06$). Peat temperature also correlated with PSN_{max} . However, the relationship was variable between the two growing seasons. In 2009, PSN_{max} decreased with warmer temperature while it increased with rising temperature in 2010. At the microform scale, hollows peat temperature explained 30 and 42 % of PSN_{max} variation during 2009 and 2010 respectively ($p < 0.001$). In the lawns and hummocks, the relationship was non-significant in 2009 ($p = 0.286$ and $p = 0.68$ respectively) but in 2010 explained 30 % of variation in the lawns ($p < 0.001$) and 32 % in the hummocks ($p < 0.001$). Q_{10} values associated with PSN_{max} were higher in 2010 in lawns and hummocks and were similar during both years in hollows which suggests that microforms with water

table >7 cm had a photosynthesis process more responsive to temperature during the 2010 season. At last, the relationship between mean CO₂ fluxes and living biomass at the end of the growing season was also analysed. Both mean seasonal respiration and PSN_{max} strongly correlated with green biomass (respectively $r^2 = 0.89$; $p = 0.001$ and $r^2 = 0.87$; $p = 0.002$).

Annual CO₂ budget

Yearly budgets represented a net loss of CO₂ to the atmosphere with greater emissions in 2009 [404 (± 287) g CO₂ m⁻² year⁻¹ compared to 272 (± 250) g CO₂ m⁻² year⁻¹ in 2010] (Table 7) (Fig. 7). Both the wintertime and growing season periods represented a net loss of CO₂ towards the atmosphere. During 2009 growing season, the peatland has lost 248 (± 248) g CO₂ m⁻² (151 days), while 124 (± 195) g CO₂ m⁻² were lost in 2010 (155 days). Mean modeled NEE in winter was similar during both years with a net loss of -150 (± 36) g m⁻² year⁻¹ in 2009 (214 days) and -150 (± 37) g m⁻² year⁻¹ in 2010 (210 day) representing 37 and 55 % of the respective annual CO₂ budget, suggesting that the interannual variation of the CO₂ balance is caused by variation of photosynthesis or respiration during the growing season.

The CO₂ balance also varied according to microforms (Table 7). Hollows remained CO₂ sinks both in 2009 and 2010 although they absorbed less in 2010 with an average NEE of 6 (± 175) g m⁻² year⁻¹ compared to 60 (± 246) g m⁻² year⁻¹ in 2009. In this microform, GPP and R decreased in 2010. Lawns represented a CO₂ source during both years with a NEE of -219 (± 483) g CO₂ m⁻² year⁻¹ in 2009 and -191 (± 404) in 2010. Both GPP and R decreased in 2010. Hummocks were also a source of CO₂ with NEE of -870 (± 589) and -546 (± 568) g m⁻² year⁻¹ in 2009 and 2010 respectively. However, during the 2010 growing season, hummocks were a small CO₂ sink with 5 (± 419) g CO₂ m⁻² absorbed between May and October. In contrast with other microforms, GPP in hummocks increased in 2010 while R decreased. Pool fluxes were larger in 2009 and contributed to 40 % of the annual spatially weighted CO₂ budget compared to 38 % in 2010.

Annual carbon balance

In order to obtain an average annual carbon balance, we modelled the Abeille peatland C balance by

Table 7 Seasonal and annual GPP, R and NEE (in g CO₂ m⁻² d⁻¹) for microforms and total ecosystem in 2009 (upper table) and 2010 (lower table)

Microforms	Winter (214)			Growing season (151)			Annual			NEE
	GPP	R	NEE	GPP	R	NEE	GPP	R	R	
Shallow pool	0	0	0	0	5.4 (0.6)	-5.4 (0.6)	0	2.2 (0.3)	2.2 (0.3)	-2.2 (0.3)
Deep pool	0	0	0	0	1.2 (0.2)	-1.2 (0.2)	0	0.5 (0.1)	0.5 (0.1)	-0.5 (0.1)
Hollows	0	0.2 (0.1)	-0.2 (0.1)	2.1 (0.2)	1.5 (1.7)	0.7 (1.5)	0.9 (0.1)	0.7 (0.8)	0.7 (0.8)	-0.2 (0.7)
Lawns	0	0.7 (0.2)	-0.7 (0.2)	4.7 (0.3)	4.9 (3.4)	-0.3 (3.1)	1.9 (0.2)	2.5 (1.5)	2.5 (1.5)	-0.6 (1.3)
Hummocks	0	2.6 (0.5)	-2.6 (0.5)	8.3 (0.7)	10.4 (3.5)	-2.1 (2.8)	3.5 (0.3)	5.9 (1.9)	5.9 (1.9)	-2.4 (1.6)
Peatland	0	0.7 (0.2)	-0.7 (0.2)	3.0 (0.2)	4.7 (1.9)	-1.6 (1.7)	1.2 (0.1)	2.4 (0.9)	2.4 (0.9)	-1.1 (0.8)
Total	0	150.8 (36.4)	-150.8 (36.4)	457.1 (35.6)	704.8 (284.1)	-247.7 (248.5)	454.1 (41.7)	858.2 (329.7)	858.2 (329.7)	-404.1 (287.9)
Microforms	Winter (210)			Growing season (155)			Annual			NEE
	GPP	R	NEE	GPP	R	NEE	GPP	R	R	
Shallow pool	0	0	0	0	3.3 (0.6)	-3.3 (0.6)	0	1.4 (0.3)	1.4 (0.3)	-1.4 (0.3)
Deep pool	0	0	0	0	0.8 (0.1)	-0.8 (0.1)	0	0.3 (0.03)	0.3 (0.03)	-0.3 (0.03)
Hollows	0	0.2 (0.1)	-0.2 (0.1)	1.6 (0.8)	1.3 (1.4)	0.3 (0.6)	0.7 (0.2)	0.7 (0.7)	0.7 (0.7)	0.02 (0.5)
Lawns	0	0.7 (0.2)	-0.7 (0.2)	3.9 (0.4)	4.1 (2.7)	-0.3 (2.3)	1.7 (0.2)	2.2 (1.3)	2.2 (1.3)	-0.5 (1.1)
Hummocks	0	2.7 (0.5)	-2.7 (0.5)	10.0 (0.9)	10.0 (3.6)	0.03 (2.7)	4.3 (0.3)	5.8 (1.8)	5.8 (1.8)	-1.5 (1.5)
Peatland	0	0.7 (0.2)	-0.7 (0.2)	3.1 (0.4)	3.9 (1.7)	-0.8 (1.3)	1.3 (0.1)	2.1 (0.8)	2.1 (0.8)	-0.8 (0.7)
Total	0	150.8 (36.3)	-150.8 (36.3)	480.3 (62.1)	604.2 (257.5)	-124.0 (195.4)	483.2 (44.9)	755.6 (295.2)	755.6 (295.2)	-272.4 (250.3)

The peatland and microforms values represent a mean daily flux while the total values represent the total flux for the season/year

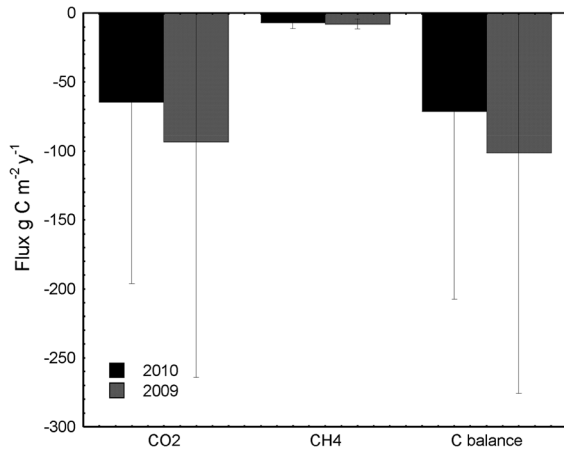


Fig. 7 CO₂, CH₄ and integrated C balance in Abeille peatland for 2009 and 2010

combining spatially weighted annual daily CO₂ fluxes measured and modelled with spatially weighted annual daily CH₄ fluxes measured in Abeille peatland during the same period. CH₄ fluxes and budget from 2009 and 2010 were described and analysed in a previous publication (Trudeau et al. 2013).

In 2009, the average spatially weighted carbon flux was $-101.2 (\pm 175)$ g C m⁻² year⁻¹ for which 92 % is accounted for CO₂-C ($93.3 (\pm 171)$ g m⁻² year⁻¹) and 11 % for CH₄-C ($7.9 (\pm 4)$ g m⁻² year⁻¹). In 2010, mean spatially weighted C flux was $-71.3 (\pm 136)$ g m⁻² year⁻¹ for which 90 % is accounted for CO₂-C ($64.5 (\pm 132)$ g m⁻² year⁻¹) and 10 % for CH₄-C ($6.8 (\pm 4)$ g m⁻² year⁻¹).

Discussion

We measured CO₂ fluxes along a microtopographical gradient in a peatland influenced by rising water table since the Little Ice Age, slowly allowing an increased pool cover and development of wet microforms (Dissanska et al. 2009; Tardif et al. 2009). 83 % of the aqualysed Abeille peatland is covered either with pools (42 %), hollows (28 %) or lawns (13 %) all of which present a mean water table higher than 7 cm. We evaluated with two years of data how these hydrologic conditions influenced the CO₂ balance at the microtopographic and ecosystem scale on this two years basis.

We observed an important variability in the fluxes at spatial and temporal scales. However, due to large

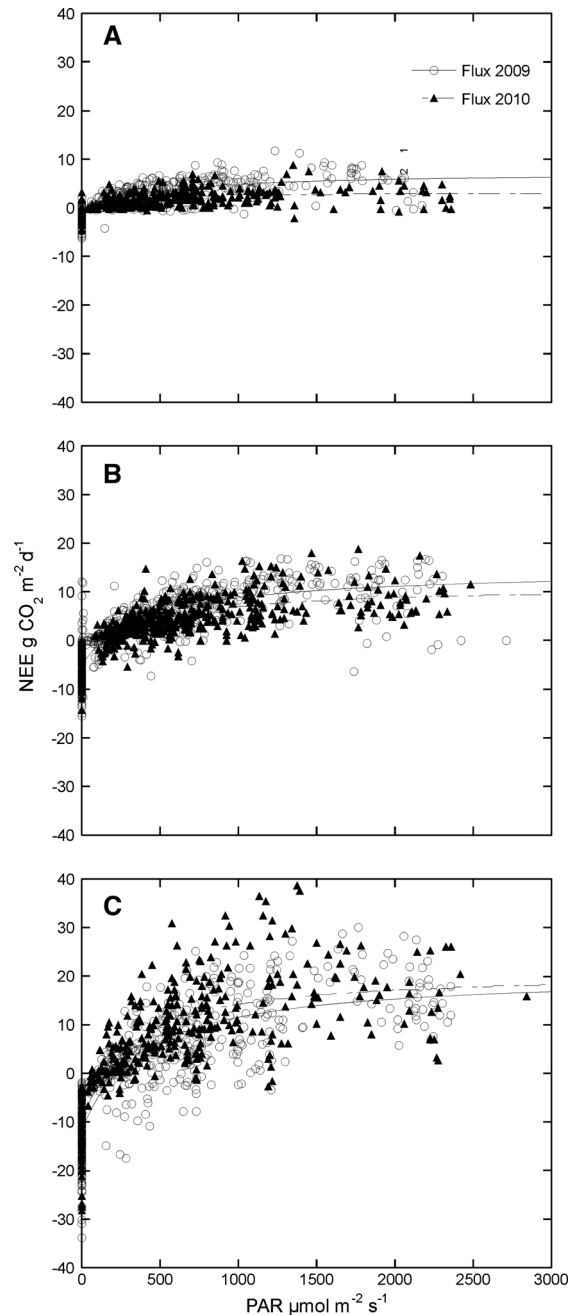


Fig. 8 Relationships between NEE and PAR for hollows (a), lawns (b) and hummocks (c) in 2009 and 2010. Points represent individual CO₂ measurements. Lines represent the curve associated to the rectangular hyperbola

measured uncertainties, it is crucial to mention that spatial and temporal variabilities discussed in this section can't be affirmed with certitude. Annual and seasonal CO₂ budgets differed between the two years,

2009 represented a large net loss to the atmosphere while 2010 was a smaller source (Fig. 7). In the terrestrial microforms, the 2009 growing season represented a net loss to the atmosphere while 2010 was a small sink (Table 7). Several studies have mentioned a switch from sink to source in the annual CO₂ budget (Shurpali et al. 1995; Joiner et al. 1999; Griffis et al. 2000; Roulet et al. 2007) and attributed the change to the hydroclimatic variability during the growing season. In the Laforge region, the 2009 growing season was dry and warm when compared to the 30-years normal (1971–2003) while 2010 was also warmer but much wetter (Fig. 3). We also observed that fluxes responded to variations in the water table and temperatures as stated by Moore and Dalva (1993), Bubier et al. (1998), Waddington et al. (1998), Updegraff et al. (2001) Strack et al. (2009). The correlation between environmental variables and fluxes varied annually and according to microtopography.

An important portion of the spatial variability of the fluxes has been linked to microtopography. GPP and R varied along a surface moisture gradient (hollow < lawn < hummock) (Figs. 8, 5, 6), which is consistent with the observed correlations between living biomass, water table and CO₂ fluxes. Nonetheless, inter-annual and intra-annual variability of NEE among the microforms indicates that they are controlled by different variables. During the 2009 and 2010 growing seasons, hollows were a CO₂ sink (Table 7). Lawns were a source both in 2009 and 2010 while hummocks were a large source in 2009 and a small sink in 2010 (Table 7). These results infer that seasonal hydro-climatic variations do influence GPP and R and vary according to microtopography. Intrinsic characteristic of the microforms such as dominant vegetation, biomass, water table depth and peat temperature play an important role in determining the fluxes.

For all the microforms of the peatland, important correlations were observed between R fluxes and peat and air temperature with warmer temperature leading to higher R fluxes (Fig. 7). Similar results were reported by Bubier et al. (2003a, 2003b) and attributed to increased decomposition. Relationship between GPP and temperature is more complex. In lawns and hummocks, warmer peat temperature did not lead to increasing rates of photosynthesis during dry periods. In June and July 2009, warmer temperature increased

R rate but did not affect photosynthesis which lead to a negative NEE (Table 7). Under wetter conditions, photosynthesis was more responsive to peat temperature than R, which lead to positive NEE in August 2009 and during the 2010 growing season (Table 7). In the hollows, photosynthesis was not reduced under dry conditions. In this microform, water table was close to peat surface during both 2009 and 2010 (3.6 cm in 2009 and 2.4 cm in 2010) and did not represent a constraint for the vegetation. Respiration and photosynthesis in the hollows showed greater response to peat and air temperature than to variation of the water table. This could explain why hollows were smaller sinks during the slightly colder 2010 while CO₂ uptake was increased in the other microforms (Table 7). It is also possible that wetter conditions of 2010 limited the capacity of vegetation to photosynthesise as it was flooded during a part of the growing season. As for pools, fluxes were reduced in 2010 in response to colder temperature and higher water table (Table 7).

Several studies have previously concluded that the CO₂ balance of peatlands is determined by temperature and surface-moisture conditions (Shurpali et al. 1995; Alm et al. 1999; Joiner et al. 1999; Griffis et al. 2000; Lafleur et al. 2001; Froelking et al. 2002; Bubier et al. 2003a; Aurela et al. 2009). In a subarctic fen near Churchill (Manitoba), Griffis et al. (2000) measured a net source of CO₂ during a hot and dry growing season and sink during warm and wet growing season. According to that study, photosynthetic activity and fitness of the vegetation is influenced by the moisture conditions during early growing season and determine the magnitude of the source/sink. Lafleur et al. (2001) also measured smaller sinks during dry growing seasons in a subarctic fen and concluded that NEE is highly sensitive to dry conditions. In a northern Finland fen, Aurela et al. (2009) measured lower CO₂ uptake during a dry and warm year which was attributed to reduced photosynthetic capacity of the vegetation.

Other authors have reported that the carbon balance response to changing climatic conditions also vary with microtopography (Alm et al. 1999; Heikkinen et al. 2002; Bubier et al. 2003a; Strack et al. 2006; Pelletier et al. 2011). Bubier et al. (2003a) suggested that the influence of the changing hydrologic conditions will vary with vegetation composition. In hummocks mainly dominated by ericaceous shrubs,

Strack et al. (2006), Bubier et al. (2003a) and Alm et al. (1999) reported lower rates of gross photosynthesis and greater respiration under dry conditions. Heikkinen et al. (2002) measured greater NEE in microsites with water table closer to peat surface while Alm et al. (1999) found that during a dry year, hollows dominated by *Sphagnum balticum* had better water retention and increased its photosynthetic capacity. In the Eastmain region (mid-boreal Québec), Pelletier et al. (2011) observed that rising water table in hummocks led to greater NEE in response to increased productivity which is consistent with our results. Moreover, this study also mentions lower photosynthesis in hollows during a wetter year which was also observed our study. This was attributed to the vegetation flooding during the 2008 wet boreal summer.

Pools also played an important role in the carbon dioxide budget. Although pool fluxes were similar to respiration in the hollows (Fig. 5c), flux direction was uniquely towards the atmosphere which generated high emission rates, similar to Hamilton et al. (1994) in a peatland complex of the Hudson Bay Lowlands. During the 2009 growing season, pools emitted $-990 (\pm 122)$ g CO₂ m⁻² (non-area-weighted) to the atmosphere while the vegetated surface emitted $-247 (\pm 1120)$ g CO₂ m⁻². In 2010, the vegetated surface represented a net sink of $11 (\pm 868)$ g CO₂ m⁻² during the growing season which was offset by pool emissions of $-631 (\pm 99)$ g CO₂ m⁻². Thus, being a constant large source of CO₂ to the atmosphere that will offset vegetated surface sink, pools are a major contributor to the overall carbon budget, especially in the context where they represent a dominant microform of a system.

Modeled winter fluxes for Abeille peatland suggest their important contribution in the annual CO₂ balance. Mean modeled fluxes for wintertime [$-0.71 (\pm 0.2)$ and $-0.72 (\pm 0.2)$ g m⁻² d⁻¹ in 2009 and 2010 respectively] (Table 7) were consistent with those of -0.69 g m⁻² d⁻¹ measured by Aurela et al. (2009) in a northern boreal fen. Mean daily winter fluxes were quite small but as the study region is characterised by long winter period (210–214 days), they represent an important part of the annual CO₂ balance particularly in hummocks, where growing season fluxes could not offset winter fluxes.

Tarnocai et al. (2002) estimated that 15 % of northeastern Canada is covered by peatlands which are

mostly represented by oligotrophic patterned fen. Pools are a predominant component of this type of peatland. Patterned fen are also observed in northern Europe (e.g. aapa mires) (Charman 2002) and peatlands of the Hudson Bay Lowlands also have large pools (Hamilton et al. 1994). Our study showed that pools contribution is non-negligible in the C balance of the peatlands. In the context where climate projections predict increased precipitations for the next decade over northeastern Canada (de Elia and Côté 2010) one can assume that these peatlands will generate important impacts in the C budget as they represent a net C source to the atmosphere.

Conclusion

Northeastern Canadian peatlands distributed at the ecotonal limit of the forest tundra and lichen woodland, showed a net carbon loss towards the atmosphere during two years of measurements. This carbon source can be explained by three main variables: meteorological conditions during the growing season, pool/vegetated surface ratio and length of the winter season.

Results show that environmental conditions during the growing season controlled C fluxes. During a dry year (2009), decreased photosynthetic activity was accompanied by increased respiration and peatland represented a net source of CO₂ both during the growing season and annually. However, this phenomenon varied according to microtopography. Microforms with water table close to surface such as hollows were less strongly influenced by drought and showed increased photosynthetic activity in 2009 in response to warmer temperature. On the other hand, the wet conditions during 2010 growing season increased photosynthesis in the hummocks and the vegetated surface represented a net CO₂ sink during the growing season.

Northeastern Canadian peatlands are mostly represented by oligotrophic patterned fens with a large pool coverage. Over the last 700 years, hydrologic changes leading to an increased water table have been registered in the region. This rise of the general water level in peatlands enhances peat decomposition on strings and degraded hummocks due to flooding and changes the pools/terrestrial surfaces ratio: 42 % of the studied peatland is covered by pools. Although mean pool CO₂ fluxes are lower than those registered in the

vegetated surface, they are unidirectional towards the atmosphere and hence play a greater role in the carbon budget of a peatland. In this study, we established that pool fluxes represent 38–40 % of the annual spatially extrapolated CO₂ fluxes.

Undergoing a subarctic climate, Northeastern Canada is characterised by short growing seasons and long winters. During the cold season, photosynthesis is inhibited but respiration fluxes are still measured. Although mean winter fluxes are rather low, the cold season represents a long period of net C loss to the atmosphere in the region and play an important role in the annual carbon budget (37–55 % in this study).

With long winters, high pool coverage and vegetated surfaces sensitive to changing meteorological conditions during the growing season, we conclude that Northeastern Canadian peatlands influenced by a hydrologic disequilibrium are and will continue to be a source of carbon, the magnitude of which will mostly be controlled by environmental conditions during the growing season.

Acknowledgments The authors would like to thank NSERC, FQRNT, Hydro-Québec and Consortium Ouranos for financial support. We gratefully thank Hans Asnong, Éric Rosa and Jean-François Hélie for judicious advices and laboratory assistance. We also thank Yan Bilodeau, Antoine Thibault, Robin Beauséjour, Sébastien Lacoste and Sylvain Jutras for field and laboratory assistance. Special thanks to Gwenael Carrer, Yann Dribault and Sandra Proulx McInnis for sharing data and results.

References

- Alm J, Schulman L, Walden J, Nykänen H, Martikainen PJ, Silvola J (1999) Carbon balance of a boreal bog during a year with an exceptionally dry summer. *Ecology* 80:161–174
- Arlen-Pouliot, Y., 2009. Développement holocène et dynamique récente des tourbières minérotrophes structurées du Haut-Boréal québécois. Thèse de doctorat, département de biologie. Université Laval, Québec
- Aurela M, Lohila A, Tuovinen J-P, Hatakka J, Riutta T, Laurila T (2009) Carbon dioxide exchange on a northern boreal fen. *Boreal Environ Res* 14:699–710
- Bubier JL, Crill PM, Moore TR, Savage K, Varner RK (1998) Seasonal patterns and controls on net ecosystem CO₂ exchange in a boreal peatland complex. *Global Biogeochem Cycles* 12:703–714
- Bubier JL, Bhatia G, Moore TR, Roulet NT, Laffleur PM (2003a) Spatial and temporal variability in growing-season net ecosystem carbon dioxide exchange at a large peatland in Ontario, Canada. *Ecosystems* 6:353–367
- Bubier JL, Crill P, Mosedale A, Frolking S, Linder E (2003b) Peatland responses to varying interannual moisture conditions as measured by automatic CO₂ chambers. *Global Biogeochem Cycles* 17:1066
- Charman D (2002) Peatlands and environmental change. Wiley, England
- Cole JJ, Caraco N (1998) Atmospheric exchange of carbon dioxide in a low-wind oligotrophic lake measured by the addition of SF₆. *Limnol Oceanogr* 43:647–656
- Cox PM, Betts RA, Jones CD, Spall SA, Totterdell IJ (2000) Acceleration of global warming due to carbon-cycle feedbacks in a coupled climate model. *Nature* 408:184–187
- Crill PM, Bartlett KB, Harriss RC, Gorham E, Verry ES, Sebacher DI, Madzar L, Sanner W (1988) Methane flux from Minnesota peatlands. *Global Biogeochem Cycles* 2:371–384
- Crusius J, Wanninkhof R (2003) Gas transfer velocities measured at low wind speed over a lake. *Limnol Oceanogr* 48:1010–1017
- de Elia R, Côté H (2010) Climate and climate change sensitivity to model configuration in the Canadian RCM over North America. *Meteorol Z* 19:325–339
- Demarty M, Bastien J, Tremblay A (2009) Carbon dioxide and methane annual emissions from two boreal reservoirs and nearby lakes in Quebec, Canada. *Biogeosci Discuss* 6:2939–2963
- Dissanska M, Bernier M, Payette S (2009) Object-based classification of very high resolution panchromatic images for evaluating recent change in the structure of patterned peatland. *Canadian Journal of Remote Sensing* 25:189–215
- Dribault Y, Chokmani K, Bernier M (2012) Monitoring seasonal hydrological dynamics of minerotrophic peatlands using multi-date GeoEye-1 very high resolution imagery and object-based classification. *Remote Sensing* 4:1887–1912
- Dyke AS, Prest VK (1987) Late Wisconsinan and Holocene history of the Laurentide ice sheet. *Géog Phys Quatern* 41:237–263
- Frolking S, Roulet N (2007) Holocene radiative forcing impact of northern peatland carbon accumulation and methane emission. *Glob Change Biol* 13:1079–1088
- Frolking S, Roulet NT, Moore TR, Laffleur PM, Bubier JL, Crill PM (2002) Modeling seasonal to annual carbon balance of Mer Bleue Bog, Ontario, Canada. *Global Biogeochemical Cycles* 16:1030
- Griffis, T.J., Rouse, W.R., Waddington, J.M., 2000. Interannual variability of net ecosystem CO₂ exchange at a subarctic fen. *Global Biogeochem Cycles* 14
- Hamilton JD, Kelly CA, Rudd JWM, Hesslein RH, Roulet NT (1994) Flux to the atmosphere of CH₄ and CO₂ from wetland ponds on the Hudson Bay lowlands (HBLs). *J Geophys Res* 99:1495–1510
- Heikkinen JEP, Elsakov V, Martikainen PJ (2002) Carbon dioxide and methane dynamics and annual carbon balance in tundra wetland in NE Europe, Russia. *Global Biogeochem Cycles* 16:1115
- Hutchinson MF, McKenney DW, Lawrence K, Pedlar JH, Hopkinson RF, Milewska E, Papadopol P (2009) Development and testing of Canada-wide interpolated spatial models of daily minimum–maximum temperature and precipitation for 1961–2003. *J Appl Meteorol Climatol* 48:725–741
- Joiner DW, Laffleur PM, McCaughey JH, Bartlett PA (1999) Interannual variability in carbon dioxide exchanges at a

- boreal wetland in the BOREAS northern study area. *J Geophys Res* 104:27663–27672
- Kling GW, Kipphut GW, Millet MC (1991) Arctic lakes and streams as gas conduits to the atmosphere: implications for tundra carbon budgets. *Science* 251:298–301
- Lafleur PM, Griffis TJ, Rouse WR (2001) Interannual variability in net ecosystem CO₂ exchange at the arctic treeline. *Arct Antarct Alp Res* 33:149–157
- MacDonald GM, Beilman DW, Kremenetski KV, Sheng Y, Smith LC, Velichko AA (2006) Rapid early development of circumarctic peatlands and atmospheric CH₄ and CO₂ variations. *Science* 314:285–288
- Macrae ML, Bello RL, Molot LA (2004) Long-term carbon storage and hydrological control of CO₂ exchange in tundra ponds in the Hudson Bay Lowland. *Hydrol Process* 18:2051–2069
- McEnroe NA, Roulet NT, Moore TR, Garneau M (2009) Do pool surface area and depth control CO₂ and CH₄ fluxes from an ombrotrophic raised bog, James Bay, Canada? *J Geophys Res* 114:G01001
- Moore TR, Dalva M (1993) The influence of temperature and water table position on carbon dioxide and methane emissions from laboratory columns of peatland soils. *Eur J Soil Sci* 44:651–664
- Moore TR, Bubier JL, Frolking SE, Lafleur PM, Roulet NT (2002) Plant biomass and production and CO₂ exchange in an ombrotrophic bog. *J Ecol* 90:25–36
- Payette S, Rochefort L (2001) *Écologie des tourbières du Québec et du Labrador*. Les Presses de l'Université Laval, Ste-Foy
- Payette S, Bhiry N, Delwaide A, Simard M (2000) Origin of the lichen woodland at its southern range limit in eastern Canada : the catastrophic impact of insect defoliators and fire on the spruce-moss forest. *Can J For Res* 30:288–305
- Pelletier L, Garneau M, Moore TR (2011) Interrannual variation in net ecosystem exchange at the microform scale in a boreal bog, Eastmain region, Quebec, Canada. *Journal of Geophysical Research*. doi:10.1029/2011JG001657
- Proulx-Mc Innis, S., 2010. Caractérisation hydrologique, topographique et géomorphologique d'un bassin versant incluant une tourbière minérotrophe fortement aqualysée, Baie-de-James, Québec. Mémoire de maîtrise, Science de l'eau. INRS, Québec
- Proulx-McInnis, S., St-Hilaire, A., Rousseau, A.N., Jutras, S., Carrer, G., Levrel, G., 2012. Seasonal and monthly hydrological budgets of a fen-dominated forested watershed, James Bay region, Quebec. *Hydrol Process* 27:1365–1378
- Roulet NT, Lafleur PM, Richard PJH, Moore TR, Humphreys ER, Bubier J (2007) Contemporary carbon balance and late Holocene carbon accumulation in a northern peatland. *Glob Change Biol* 13:397–411
- Shurpali NJ, Verma SB, Kim J, Arkebauer TJ (1995) Carbon dioxide exchange in a peatland ecosystem. *J Geophys Res* 100:14319–14326
- Silvola J, Alm J, Ahlholm U, Nykanen H, Martikainen PJ (1996) CO₂ fluxes from peat in boreal mires under varying temperature and moisture conditions. *J Ecol* 84:219–228
- Strack M, Price JS (2009) Moisture controls on carbon dioxide dynamics of peat-*Sphagnum* monolith. *Ecohydrology* 2:34–41
- Strack M, Waddington JM, Rochefort L, Tuittila ES (2006) Response of vegetation and net ecosystem carbon dioxide exchange at different peatland microforms following water table drawdown. *J Geophys Res* 111:G02006
- Strack M, Waddington JM, Lucchese MC, Cagampan JP (2009) Moisture controls on CO₂ exchange in a *Sphagnum*-dominated peatland: results from an extreme drought field experiment. *Ecohydrology* 2:454–461
- Tardif S, St-Hilaire A, Roy R, Bernier M, Payette S (2009) Statistical properties of hydrographs in minerotrophic fens and small lakes in mid-latitude Québec, Canada. *Canadien Water Resour J* 34:365–380
- Tarnocai C, Kettles IM, Lacelle B (2002) Peatlands of Canada database. Natural Resources Canada, Ottawa
- Trudeau N, Garneau M, Pelletier L (2013) Methane fluxes from a patterned fen of the northeastern part of the La Grande river watershed, James Bay, Canada. *Biogeochemistry* 113:409–422
- Ullah S, Frasier R, Pelletier L, Moore TR (2009) Greenhouse gas fluxes from boreal forest soils during the snow-free period in Quebec, Canada. *Can J For Res* 3:666–680
- Updegraff K, Bridgham SD, Pastor J, Weishampel P, Harth C (2001) Response of CO₂ and CH₄ emissions from peatlands to warming and water table manipulation. *Ecol Appl* 11:311–326
- Van Bellen S, Garneau M, Ali AA., Lamarre A., Robert EC, Magnan G, Asnong H, Pratte S (2013) Poor fen succession over ombrotrophic peat related to late-Holocen increased surface wetness in subarctic Quebec, Canada. *J Quat Sci* 28:748–760
- Waddington JM, Roulet NT (1996) Atmosphere-wetland carbon exchanges: scale dependency of CO₂ and CH₄ exchange on the developmental topography of a peatland. *Global Biogeochem Cycles* 10:233–245
- Waddington JM, Griffis TJ, Rouse WR (1998) Northern canadian wetlands: net ecosystem CO₂ exchange and climatic change. *Climatic Change* 40:267–275
- Yu Z, Loisel J, Brosseau DP, Beilman DW, Hunt SJ (2010) Global peatland dynamics since the Last Glacial Maximum. *J Geophys Res Lett* 37:L13402